THREE DIMENSIONAL THEORY AND SIMULATION OF AN ELLIPSE-SHAPED CHARGED-PARTICLE BEAM GUN*

R. Bhatt, T. Bemis, and C. Chen
Plasma Science and Fusion Center, MIT, Cambridge, MA 02139

Abstract

A three-dimensional (3D) theory of non-relativistic, laminar, space-charge-limited, ellipse-shaped, charged-particle beam formation has been developed recently [1] whereby charged particles (electrons or ions) are accelerated across a diode by a static voltage differential and focused transversely by Pierce-type external electrodes placed along analytically specified surfaces. The treatment is extended to consider whether the diode geometry solutions thus obtained are robust to perturbations and limitations of the sort likely to be encountered in a realistic device: finite extent, part misalignment, tolerances for mechanical and thermal stresses, etc. Analytic and semi-analytic estimates are presented along with simulations utilizing the 3D trajectory code, OMNITRAK [2]. It is found that the elliptic-beam solution is quite stable and robust, and its desirable properties can be maintained in a realistic diode.

INTRODUCTION

Electron beams of elongated elliptic cross-sections have generated great interest in vacuum electronics, because of their low space-charge energy and efficient coupling to rf structures when compared to circular beams. It is well-known that high space-charge reduces conversion efficiency in conventional microwave tubes employing circular beams. Presently, there are vigorous activities in the development of sheet-beam traveling wave amplifiers [3,4], klystrons [5], and focusing systems [6,7].

In high-intensity ion and electron accelerators, beams often exhibit non-laminar flows such as large-amplitude density fluctuations, mismatched envelope oscillations, emittance growth, chaotic particle orbits, beam interception, and difficulty in beam focusing and compression. Many of these effects are due to beam mismatch or non-equilibrium behavior. Elliptic beams may allow simplified and more natural matching [8] between beam injectors and commonly used magnetic focusing lattices, reducing the emittance growth associated with beam mismatch.

Although elliptic beams present numerous advantages, their inherent three-dimensional nature has made diode design a challenging process, both analytically and numerically. For the applications discussed above, desirable beam characteristics include uniform current density, parallel flow, and zero magnetic flux threading the emitter – properties consistent with one-dimensional Child-Langmuir [9] flow, in which the electrostatic potential varies as $\Phi \propto z^{4/3}$, where z is the beam propagation distance. In general, however, such flows are difficult to produce. Recent studies of 2D and 3D extensions of the Child-Langmuir law in an infinite applied magnetic field have shown that the beam exhibits significant current density enhancements near the beam-vacuum boundary. In the absence of an infinite confining magnetic field, the beam will tend to spread in phase-space, resulting in a degradation of beam quality. As shown in Ref. [1], it is possible to induce the space-charge flow in a 3D system to take the 1D Child-Langmuir flow form by calculating a 3D equipotential geometry that is consistent with the 1D Child-Langmuir electric field within the beam and constructing external electrodes lying along the equipotentials as prescribed that focus the beam. Such a beam can, in theory, exhibit extremely low emittance, laminar flow.

The equipotential surfaces calculated using the methods of Ref. [1], however, are idealizations, and it is an important question whether the solutions thus obtained are robust to perturbations and limitations of the sort likely to be encountered in a realistic device: finite extent, part misalignment, tolerances for mechanical and thermal stresses, etc. Analytic and semi-analytic estimates are presented along with 3D simulations utilizing the 3D trajectory code, OMNITRAK [2], and it is found that the elliptic-beam solution is quite stable and robust, and its desirable properties can be maintained in a realistic diode.

ELLIPTIC GUN GEOMETRY

We consider a non-relativistic charged-particle beam of length d and elliptic cross-section with semi-major axis a and semi-minor axis b, as shown in Fig. 1. The charged particles are emitted from a flat elliptic plate, held at potential $\Phi = 0$, in the $z = 0$ plane and collected by another flat elliptic plate, held at potential $\Phi = \Phi_d$, in the $z = d$ plane. The cold fluid equations describing the beam interior are $\nabla^2\Phi = -4\pi qn$, $\partial n/\partial t + \nabla \cdot (n\mathbf{V}) = 0$, and $\partial \mathbf{V}/\partial t + (\mathbf{V} \cdot \nabla)\mathbf{V} = -(q/m)\nabla\Phi$, for the region $x^2/a^2 + y^2/b^2 \le 1$ and $0 \le z \le d$. In these equations, $\mathbf{V}$ is the flow velocity, and n is the density of particles, each of mass m and charge q. Note that, consistent with the non-relativistic approximation, we neglect any self-magnetic field. In the beam exterior, the potential satisfies Laplace's equation, $\nabla^2\Phi = 0$.

* Work supported by the U.S. Department of Energy, High-Energy Physics Division, Grant No. DE-FG02-95ER40919, Office of Fusion Energy Science, Grant No. DE-FG02-01ER54662, Air Force Office of Scientific Research, Grant No. F49620-03-1-0230, and the MIT Deshpande Center for Technological Innovation.

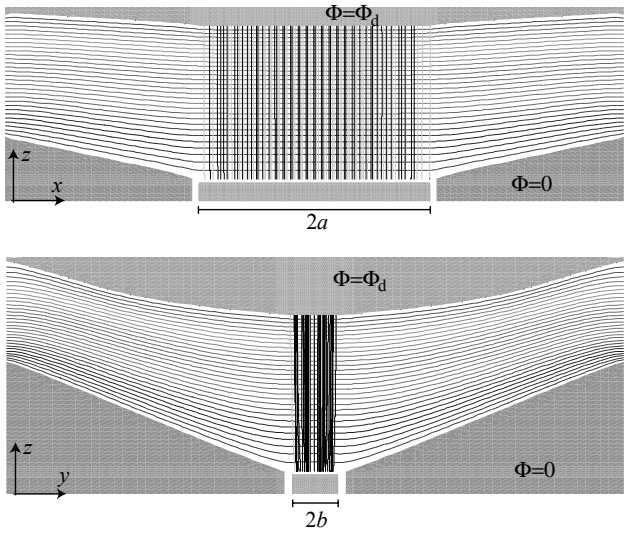

Figure 1: Elliptic charged-particle beam diode shown in the *x*-*z* and *y*-*z* planes. The beam has semi-major axis *a* and semi-minor axis *b*, emitted at potential $\Phi = 0$ and collected at potential $\Phi = \Phi_d$ after propagating a distance *d* along $\hat{\mathbf{e}}_z$.

The 1D steady-state solution to the interior problem defined by the cold fluid equations can be obtained by using the plate potentials as boundary conditions for Poisson's equation and imposing the constraint that particles emerge from the $\Phi = 0$ emitter with zero velocity, i.e. the space-charge-limited boundary condition. This results in the well-known 1D Child-Langmuir (C-L) [12] solution for laminar, space-charge-limited flow with $\mathbf{V}(z) = \hat{\mathbf{e}}_z (2q\Phi_d/m)^{1/2}(z/d)^{2/3}$, $n(z) = (\Phi_d/9\pi q d^2)(z/d)^{-2/3}$, and $\Phi(z) = \Phi_d (z/d)^{4/3}$. For example, an electron diode of length $d = 4.11\,\text{mm}$ and diode voltage $\Phi_d = 2.29\,\text{kV}$ produces a current density of $1.51\,\text{A/cm}^2$.

A 3D cold-beam space-charge-limited emission simulation using the commercially-available ray-tracing code OMNITRAK is shown in Fig. 1 for a 6:1 elliptic beam using the example parameters $a = 3.73\,\text{mm}$ and $b = 0.62$ mm. A variable-resolution computational mesh is employed with x-spacing of 0.05 mm for $0 \le x \le 4$ mm and 0.05 mm for $4 \le x \le 10$ mm, y-spacing of 0.05 mm for $0 \le y \le 1$ mm and 0.2 mm for $1 \le y \le 8$ mm, and z-spacing of 0.05 mm for $0 \le z \le 0.4$ mm and 0.1 mm for $0.4 \le z \le 10$ mm. The mesh resolution is higher in x and y across the cross-section of the beam, and in z where the beam leaves the emitter as shown in Fig. 1. Nearby computational nodes are shifted to conform to the electrode surfaces using the OMNITRAK *surface* flag. Neumann boundaries were used for the symmetry planes of the beam as well as for the outer boundaries of the mesh, which is shown in Fig. 1 along with computed equipotentials and particle trajectories projected to the $x = 0$ and $y = 0$ planes. The entire simulation runs in approximately 30 minutes on a 3 GHz personal computer.

The beam produced by the simulation is essentially parallel, laminar, uniform density Child-Langmuir flow. Beam laminarity is often characterized by the rms beam emittances $\varepsilon_x \equiv \left(\langle x^2\rangle\langle x'^2\rangle - \langle xx'\rangle^2\right)^{1/2}$ and $\varepsilon_y \equiv \left(\langle y^2\rangle\langle y'^2\rangle - \langle yy'\rangle^2\right)^{1/2}$, where the averages of transverse particle position (x, y) and divergence $(x', y') \equiv (dx/dz, dy/dz)$ are taken over a slice of the beam at $z = d$. For a uniform density elliptic beam, these emittances can be related to effective beam temperatures [10] by the relations $\varepsilon_x = a\left(kT_{eff,x}/8q\Phi_d\right)^{1/2}$ and $\varepsilon_y = b\left(kT_{eff,y}/8q\Phi_d\right)^{1/2}$. Using the example parameters of Fig. 1, the OMNITRAK simulation shown predicts the effective beam temperatures $T_{eff,x} = 280\,\text{K}$ and $T_{eff,y} = 1700\,\text{K}$.

PARAMETRIC ROBUSTNESS

The effective beam temperatures of the previous section are not meaningful in practice beyond their use as a measure of the minimum beam temperature growth associated with the gun optics.

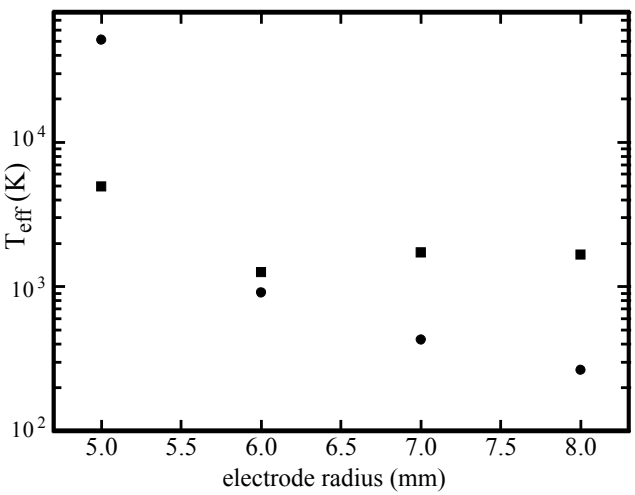

Figure 2: The effective beam temperature T_{eff} is plotted as the termination radius of the beam-focusing electrodes is varied. The circles indicate $T_{eff,x}$, while the squares indicate $T_{eff,y}$.

The theory of Ref. [1] computes equipotentials extending infinitely far from the beam. In practice, electrodes lying along these equipotentials will have a finite length, and it is important to assess the impact of the edge effects thus admitted on the beam. Since the potential satisfies Laplace's equation in the free-space region outside the beam, we expect that electrostatic potential variations caused by localized perturbations of the electrode geometry will be exponentially decaying with distance from the perturbation point. We test this hypothesis by performing several cold-beam OMNITRAK simulations where the radial extent of the electrodes is

varied, while the Neumann boundaries at the edge of the simulation region are kept constant. The effective beam temperatures at the anode are shown as a function of electrode radius in Fig. 2. We see that the influence of electrode structure beyond 6mm in radius is minimal.

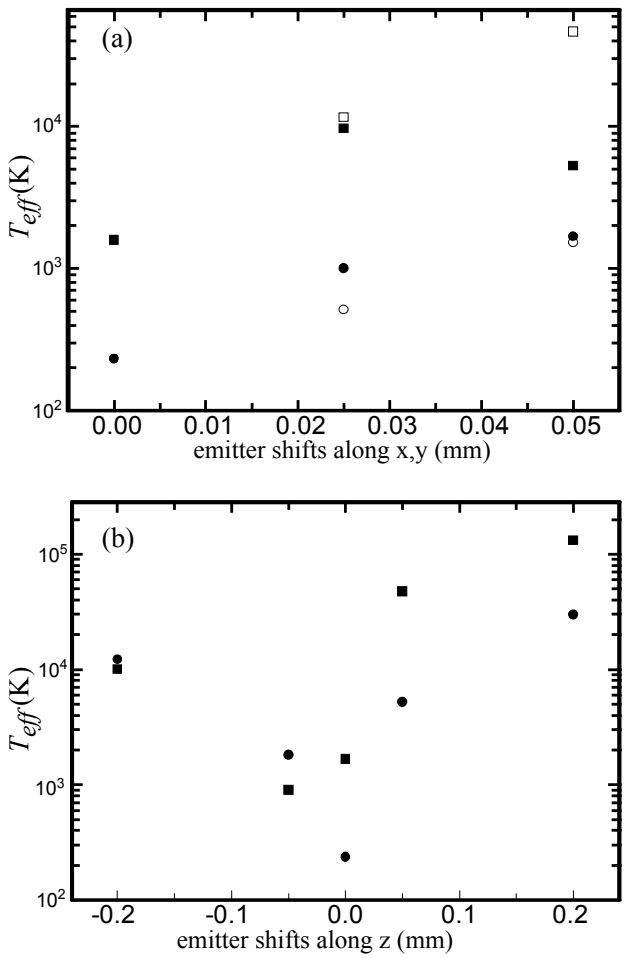

Figure 3: The effective beam temperature, T_{eff} is plotted as the emitter is shifted (a) in the transverse *x*-*y* plane and (b) in *z*. The circles indicate $T_{eff,x}$, while the squares indicate $T_{eff,y}$. In (a), the solid circles and squares represent shifts along *x*, while the open circles and squares represent shifts along *y*.

While the electrode length study establishes the insensitivity of the beam quality to geometry perturbations far from the beam, we must allow for machining tolerances in the cutting and alignment of parts close to the beam as well. Several cold-beam OMNITRAK simulations were performed with small shifts in the emitter stalk position, and results are shown in Fig. 3. The greatest sensitivity is observed with respect to transverse misalignments – precise emitter positioning within 0.02 mm is desirable to minimize beam temperature growth.

A hot thermionic emitter is often thermally isolated from the focus electrode by a vacuum gap. We vary the elliptical gap width by a single parameter, δ_g, which represents the difference between the semi-major/minor radii of the inner edge of the focus electrode and the semi-major/minor radii of the emitter, and show the results in Fig. 4.

As expected, for large values of the gap, the electrodes no longer impose the proper boundary conditions on the beam edge, and thus emittance growth is seen. We find that, a gap thickness greater than 0.05 – 0.1 mm would not be desirable.

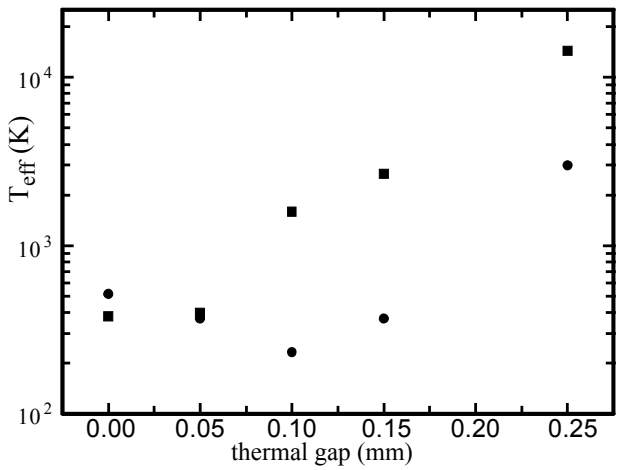

Figure 4: The effective beam temperature, T_{eff} is plotted as the vacuum gap thickness δ_g around the emitter is varied. The circles indicate $T_{eff,x}$, while the squares indicate $T_{eff,y}$.

CONCLUSION

The sensitivity of the electrode specification theory of Ref [1] to physical geometry and machining limitations such as finite extent, part misalignment, and tolerances for mechanical and thermal stresses is established. The greatest sensitivity is seen to transverse misalignments of the emitter stalk.

REFERENCES

[1] R. Bhatt and C. Chen, Phys. Rev. ST Accel. Beams 8, 104201 (2005).
[2] OMNITRAK software, copyright Field Precision, Albuquerque, NM.
[3] S. Humphries, S. Russell, B. Carlsten, and L. Earley, Phys. Rev. ST AB 7, 060401 (2004).
[4] B.E. Carlsten, Phys. Plasmas 9, 5088 (2002).
[5] G. Caryotakis, et al., AIP Conference Proceedings 691, 22 (2003).
[6] M.A. Basten and J.H. Booske, J. Appl. Phys. 85, 6313 (1999).
[7] R. Pakter and C. Chen, Phys. Rev. E 62, 2789 (2000).
[8] C. Chen. R. Pakter, and R.C. Davidson, Nucl. Inst. And Methods A 464, 518 (2001).
[9] C.D. Child, Phys. Rev. 32, 492 (1911); I. Langmuir, ibid. 21, 419 (1923).
[10] F. Zhou, et al., Phys. Rev. ST Accel Beams 5, 094203 (2003).